Resolution of two apparent paradoxes concerning quantum oscillations in underdoped high-T_c superconductors

Xun Jia,[1] Pallab Goswami,[2] and Sudip Chakravarty[1]
[1]*Department of Physics and Astronomy, University of California–Los Angeles, Los Angeles, California 90095-1547, USA*
[2]*Department of Physics and Astronomy, Rice University, Houston, Texas 777005, USA*
(Received 20 April 2009; revised manuscript received 4 June 2009; published 6 October 2009)

Recent quantum-oscillation experiments in underdoped high-temperature superconductors seem to imply two paradoxes. The first paradox concerns the apparent nonexistence of the signature of the electron pockets in angle-resolved photoemission spectroscopy (ARPES). The second paradox is a clear signature of a small electron pocket in quantum-oscillation experiments, but no evidence as yet of the corresponding hole pockets of approximately double the frequency of the electron pocket. This hole pockets should be present if the Fermi-surface reconstruction is due to a commensurate density wave, assuming that Luttinger sum rule relating the area of the pockets and the total number of charge carriers holds. Here we provide possible resolutions of these apparent paradoxes from the commensurate *d*-density wave theory. To address the first paradox we have computed the ARPES spectral function subject to correlated disorder, natural to a class of experiments relevant to the materials studied in quantum oscillations. The intensity of the spectral function is significantly reduced for the electron pockets for an intermediate range of disorder correlation length, and typically less than half the hole pocket is visible, mimicking Fermi arcs. Next we show from an exact transfer-matrix calculation of the Shubnikov-de Haas oscillation that the usual disorder affects the electron pocket more significantly than the hole pocket. However, when, in addition, the scattering from vortices in the mixed state is included, it wipes out the frequency corresponding to the hole pocket. Thus, if we are correct, it will be necessary to do measurements at higher magnetic fields and even higher-quality samples to recover the hole-pocket frequency.

DOI: 10.1103/PhysRevB.80.134503 PACS number(s): 74.25.Jb, 74.25.Ha, 74.72.Bk

I. INTRODUCTION

High-temperature superconductors have been addressed from a remarkable number of vantage points. Nonetheless many of the basic questions still remain unresolved and the notion of broken symmetries arising from a Fermi liquid has been traditionally discarded in favor of many exotic ideas. Here we revisit the Fermi-liquid concept and a particular broken symmetry in response to a class of recent quantum-oscillation experiments.[1–6] We and others[7–13] have had some success in this respect. If these theories and experiments are correct, one will have to radically alter our 20 year-old view of these superconductors.[14] The totality of phenomenology cannot of course be explained without serious Fermi-liquid corrections. But as long as the quasiparticle residue is finite, we hope that the low-energy properties can be understood from our perspective.

Two paradoxes have arisen in the context of the quantum-oscillation measurements. The first is the contrast between Fermi arcs observed in angle-resolved photoemission (ARPES) experiments[15] on one hand and recent quantum-oscillation experiments suggesting small Fermi pockets in underdoped $YBa_2Cu_3O_{6+\delta}$ (YBCO),[1–6] on the other. This is particularly clear in recent ARPES experiments where an effort was made to examine YBCO with similar doping as in the quantum-oscillation measurements.[16]

The second paradox is the nonexistence of any evidence of the hole pockets in quantum-oscillation measurements. Within the density wave scenario of wave vector $\mathbf{Q}=(\pi,\pi)$ (the lattice spacing set to unity), there should be two dominant frequencies in quantum oscillations. One corresponding to the electron pocket at about 500 T and the other corresponding to the hole pocket at around 900 T. These are of course rough numbers corresponding to approximately 10% doping, assuming that the Luttinger sum rule is satisfied in the mixed state, that is, the quantum oscillations reflect the normal state even if the measurements may lie within the mixed state.

The concept of a broken symmetry is very powerful because deep inside a phase a physically correct effective Hamiltonian can address many important questions, whereas our inability to reliably predict properties of even a single-band Hubbard model, while widely pursued, has been a limiting factor. This is not an empty exercise, if new phenomena can be predicted or striking facts can be explained with some degree of simplicity. That broken symmetry both dictates and protects the nature of elementary excitations, determining the properties of matter, is important to emphasize.

The suggested form of order, the *d*-density wave (DDW),[17] explains numerous properties of these superconductors, including the concomitant suppression of the superfluid density,[18] Hall number,[19] and more recently the large enhancement of Nernst effect in the pseudogap state,[20] in addition to the existence of a single-particle gap of $d_{x^2-y^2}$ form above T_c. There are also theoretical reasons why DDW is a possibility. It competes favorably with other ordering tendencies in variational studies of extended Hubbard models with nearest-neighbor repulsion and pair-hopping terms.[21,22] It is also realized in a class of two-leg ladder models with nearest-neighbor repulsion.[23] However, whatever form the correct Hamiltonian takes, we know that it must favor *d*-wave superconductivity (DSC). Such a Hamiltonian will almost certainly favor DDW order as well in light of the abundance of local Hamiltonians which do not dis-

criminate between DSC and DDW order. In fact, two carefully designed difficult polarized neutron-scattering experiments have provided tantalizing direct evidence of DDW order,[24,25] although other experiments have claimed otherwise.[26–28]

A natural enemy of the pristine properties of matter is disorder that is unavoidable in complex systems such as high-temperature superconductors. The role of disorder was emphasized in the original proposal of DDW order as a relevant competing order in the phase diagram of high-T_c superconductors,[17] although our views of disorder have greatly evolved during the intervening years. It is this DDW order combined with disorder that would be the focus of the present paper in resolving the paradoxes stated above. The disorder considered are of two different types: (1) scattering due to impurities and defects and (2) scattering from vortices in the mixed states.

We consider two kinds of intrinsic disorder: (a) Gaussian white noise and (b) correlated disorder with a finite correlation length. In the momentum space the scattering rate for correlated disorder will decay as $\exp(-q^2 l_D^2)$, where $\mathbf{q}$ is the momentum transfer between the initial and the final states, l_D being the correlation length. Therefore, because of its smaller size, the states corresponding to the electron pockets are scattered more than on the hole pockets. This is an interpretation of the phenomenon and is based on intrapocket scattering. An alternative interpretation involves the density of states on the Fermi surface of the electron pockets. In contrast, for white noise, scattering is independent of momentum and affects both pockets similarly. Disorder naturally has a strong effect on ARPES spectral function, which is sensitive to the coherence factors that are analogs of Wannier functions. In Shubnikov-de Haas (SdH) oscillations it is only the averaged effect of disorder that enters by determining the effective lifetime on the Fermi surface. Therefore, the role of disorder is quite different, as we shall explicitly see.

Correlated disorder is also experimentally relevant. Unlike quantum-oscillation experiments which probes bulk properties, ARPES is inherently a surface probe. In the relevant case of YBCO, as cleaved surfaces show that CuO and BaO terminations give different contributions to the total photoemission intensity, with a hole doping $n_h=30\%$, almost irrespective of the nominal bulk doping. This self-doping was controlled by evaporating potassium *in situ* on the cleaved surface, so as to reduce the hole content down to the value of underdoped bulk YBCO ($\delta \approx 0.5$),[16] the doping level for which many quantum-oscillation experiments are carried out. The potassium overlayer is likely to produce an effective correlated disorder in the CuO plane.

To explain the second paradox we shall adapt an analysis of Stephen[29] to include a normal state that exhibits DDW order. We shall see that the relativistic character of the nodal fermions of the hole pocket, as opposed to the nonrelativistic nature of the charge carriers of the electron pocket provides a possible explanation. If we denote the Dingle factor of the electron pocket by $\mathcal{D}_e = e^{-\pi/\omega_c \tau_v}$, the Dingle factor of the hole pocket is $\mathcal{D}_h \approx \mathcal{D}_e^{4.4}$. This huge suppression may be the resolution of the missing frequency from the hole pocket. Here, ω_c is the cyclotron frequency corresponding to the electron pocket and $1/\tau_v$ is the scattering rate of the electrons from the vortices in the mixed state. The analysis of Stephen also leads to a tiny shift of the relative frequency of the quantum oscillations in the mixed state, on the order of 10^{-6}. Thus, there is enough leeway that even a very large error in this estimate will not affect our conclusions.

The organization of the paper is as follows. In Sec. II we compute the ARPES spectral function and show that disorder can destroy the evidence of electron pockets. Section III is devoted to an exact transfer-matrix computation of Shubnikov-de Haas oscillations and the effect of disorder on it. Section IV contains a discussion of scattering of quasiparticles of the putative normal state from the vortices in the mixed state. In Sec. V we briefly summarize the salient features of our work.

II. SPECTRAL FUNCTION

A. Hamiltonian

The Hamiltonian of commensurate DDW order in terms of the fermion creation and destruction operators, $c_{\mathbf{k}}^\dagger$ and $c_{\mathbf{k}}$, in the momentum space is

$$H_1 = \sum_{\mathbf{k}\in \mathrm{RBZ}} (\epsilon_{\mathbf{k}} c_{\mathbf{k}}^\dagger c_{\mathbf{k}} + \epsilon_{\mathbf{k}+\mathbf{Q}} c_{\mathbf{k}+\mathbf{Q}}^\dagger c_{\mathbf{k}+\mathbf{Q}}) + \sum_{\mathbf{k}\in \mathrm{RBZ}} (i W_{\mathbf{k}} c_{\mathbf{k}}^\dagger c_{\mathbf{k}+\mathbf{Q}} + \mathrm{H.c.}), \quad (1)$$

where the ordering wave vector $\mathbf{Q}=(\pi,\pi)$ and $\epsilon_{\mathbf{k}}$ is the single-particle spectra. The lattice constant is set to be unity for simplicity. The reduced Brillouin zone is bounded by $k_y \pm k_x = \pm \pi$. We define $\epsilon_{\mathbf{k}}$ by

$$\epsilon_{\mathbf{k}} = -2t(\cos k_x + \cos k_y) + 4t' \cos k_x \cos k_y - 2t''(\cos 2k_x + \cos 2k_y) \quad (2)$$

and the DDW gap by

$$W_{\mathbf{k}} = \frac{W_0}{2}(\cos k_x - \cos k_y). \quad (3)$$

B. Disorder

Potential disorder in real space with a finite correlation length l_D is modeled by

$$V(\mathbf{r}) = \frac{g_V}{2\pi l_D^2} \int d\mathbf{x}\ e^{-|\mathbf{r}-\mathbf{x}|^2/2l_D^2} G(\mathbf{x}), \quad (4)$$

where the disorder averages are $\langle G(\mathbf{x})\rangle = 0$ and $\langle G(\mathbf{x})G(\mathbf{y})\rangle = \delta(\mathbf{x}-\mathbf{y})$; the disorder intensity is set by g_V. This disorder Hamiltonian in the momentum space is then

$$H_2 = \sum_{\mathbf{k}_1,\mathbf{k}_2\in \mathrm{BZ}} V(\mathbf{k}_1,\mathbf{k}_2) c_{\mathbf{k}_1}^\dagger c_{\mathbf{k}_2} + \mathrm{H.c.}, \quad (5)$$

where the matrix elements are

$$V(\mathbf{k},\mathbf{k}+\mathbf{q}) = \frac{g_V}{2\pi} e^{-q^2 l_D^2/2} u(\mathbf{q}), \quad (6)$$

and $u(\mathbf{q})$ is

$$u(\mathbf{q}) = \frac{1}{2\pi}\int d\mathbf{y}\ \ G(\mathbf{y})e^{-i\mathbf{q}\cdot\mathbf{y}}, \tag{7}$$

satisfying the conditions of $\langle u(\mathbf{q})\rangle = 0$ and $\langle u(\mathbf{q})u(\mathbf{q}')\rangle = \delta(\mathbf{q}+\mathbf{q}')$. In practice, we generate $u(\mathbf{q})$ directly with the desired statistical properties and then compute the matrix elements in Eq. (5).

C. Computation of ARPES spectral function

Once the full Hamiltonian $H=H_1+H_2$ is generated, it is diagonalized by the transformation $c_{\mathbf{k}}=\Sigma_l P_{\mathbf{k},l}\gamma_l$, where γ_l is the annihilation operator of quasiparticles with energy E_l. The coefficients $P_{\mathbf{k},l}$ and energy E_l are obtained through an exact numerical diagonalization procedure. Finally, the ARPES spectral function $A(\mathbf{k},\omega)$ at a temperature T is given by

$$A(\mathbf{k},\omega) = 2\pi\sum_l |P_{\mathbf{k}l}|^2 n_l \delta(\omega - E_l), \tag{8}$$

where $n_l = 1/\{1+\exp[(E_l-\mu)/k_BT]\}$ is the fermion occupation number. Note that the numerical implementation of Eq. (8) requires an approximation of the delta function by, for example, a Lorentzian distribution.

We discretize the Brillouin zone with a mesh of size 80×80, and diagonalize the corresponding Hamiltonian. The parameters we choose for YBCO at 10% doping are: $t=0.3$ eV, $t'=0.3t$, $t''=t'/9.0$, and $W_0=0.0825$ eV, same as before.[7] The chemical potential μ is set to be -0.2627 eV. These parameters yield a hole doping of $n_h \sim 10\%$. The temperature $T=10$ K is chosen, where a typical ARPES experiment is performed. For $g_V/(2\pi)=0.1t$, the quasiparticle lifetime for $l_D=0$ is of the order $\tau \sim 10^{-12}$ s from Fermi's golden rule, which is a reasonable value.[3,6] Note that the bandwidth is $8t$. The scattering rate for correlated disorder for a finite $l_D \sim 4$ is considerably smaller, as can be seen from Eq. (6). The final spectral function is obtained by averaging over 20–50 disorder configurations until no difference is detected upon further averaging. A typical result with disorder correlation length $l_D=4$, in units of the lattice constant, is plotted in Fig. 1. The electron pockets are barely visible, resembling experimental observations. From Fermi's golden rule, the scattering rate is proportional to the square of the matrix element between the initial and the final states, $V(\mathbf{k},\mathbf{k}+\mathbf{q}) \sim \exp(-q^2 l_D^2/2)$ [see Eq. (6)], where $\mathbf{q}$ is the momentum transfer in the scattering process. On average, the scattering rate is therefore proportional to $\exp(-q_t^2 l_D^2/2)$, where q_t is a typical momentum transfer. In particular, q_t is roughly the size of a pocket. Because electron pockets are much smaller than hole pockets, the scattering rate is greater for electron pockets. The hole pockets centered at $(\pm\pi/2, \pm\pi/2)$ have vanishingly small spectral function on the back side due to the coherence factors and appear as Fermi arcs instead,[30] whose lengths are further reduced by disorder.

We also demonstrate the dependence of the spectral function $A(\mathbf{k},\omega=\mu)$ on l_D in Fig. 2. The disorder correlation lengths are $l_D=0$, 2, 8, and 16 for panels (a) through (d), respectively. There are three distinct regimes depending on

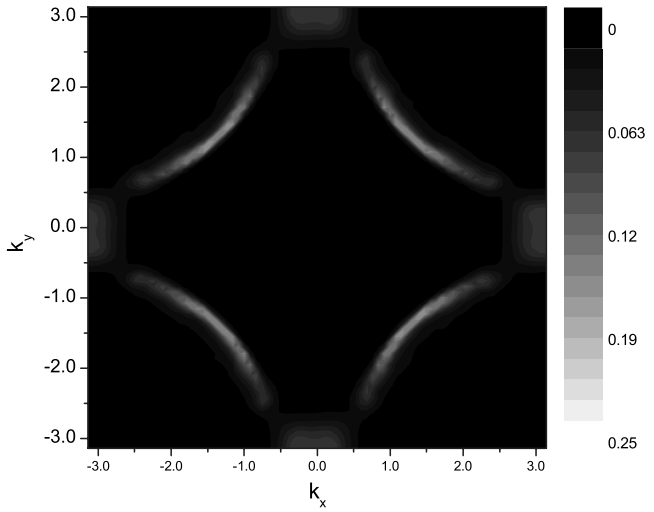

FIG. 1. The spectral function $A(\mathbf{k},\omega)$ at $\omega=\mu$ with correlated disorder corresponding to $l_D=4$. The remaining parameters are stated in the text.

l_D. For small l_D, the electron and hole pockets will be almost equally scattered. As a consequence, the spectral function is smeared out everywhere; see Fig. 2(a). For intermediate values of l_D, for example, $l_D=2$ in Fig. 2(b) and $l_D=4$ in Fig. 1, scattering is more prominent for electron pockets, resulting in a picture consisting of only four Fermi arcs. Finally, as the correlation length l_D increases further, Figs. 2(c) and 2(d), the electron pockets reappear. Indeed, though more disorder scattering occurs on the electron pockets, the spatial variation in disorder, hence the net effect of disorder, becomes weaker.

To characterize the energy dependence of the spectral function, we compute $A(\mathbf{k},\omega)$ as a function of ω at two $\mathbf{k}$ points in the Brillouin zone. One of them is at the intersection ΓY line with the inner side of the Fermi surface, the other is situated on the electron pocket along the direction ΓM; see Fig. 3. The disorder correlation length was chosen to be $l_D=4$. Although there are peaks at $\omega \sim \mu$ for both, the peak corresponding to the electron pocket is significantly suppressed by disorder; the second peak at $\omega-\mu \sim -0.2$ eV is clearly an artifact of our simple theory and such high-energy states would surely decay once correlation effects are taken into account by the creation of particle-hole pairs.

In Fig. 4, $A(\mathbf{k},\omega)$ is plotted as a function of both $\mathbf{k}$ and ω. The horizontal axis is along the path $\Gamma \to Y \to M \to \Gamma$ in the Brillouin zone. The spectral function is negligibly small outside the reduced Brillouin zone bounded by $k_x \pm k_y = \pm\pi$,[30] and consequently there are no peaks in the central region of Fig. 4. Close to $\mathbf{k}=(\pi,0)$ and $\omega=\mu$, $A(\mathbf{k},\omega)$ has very small intensity due to long-range correlated disorder, consistent with our previous observation that the electron pockets are most likely unobservable.

III. SHUBNIKOV-DE HAAS OSCILLATIONS

A. The transfer-matrix method

Let us now consider the effect of disorder on SdH oscillations of the conductivity, σ_{xx}. The tight-binding Hamil-

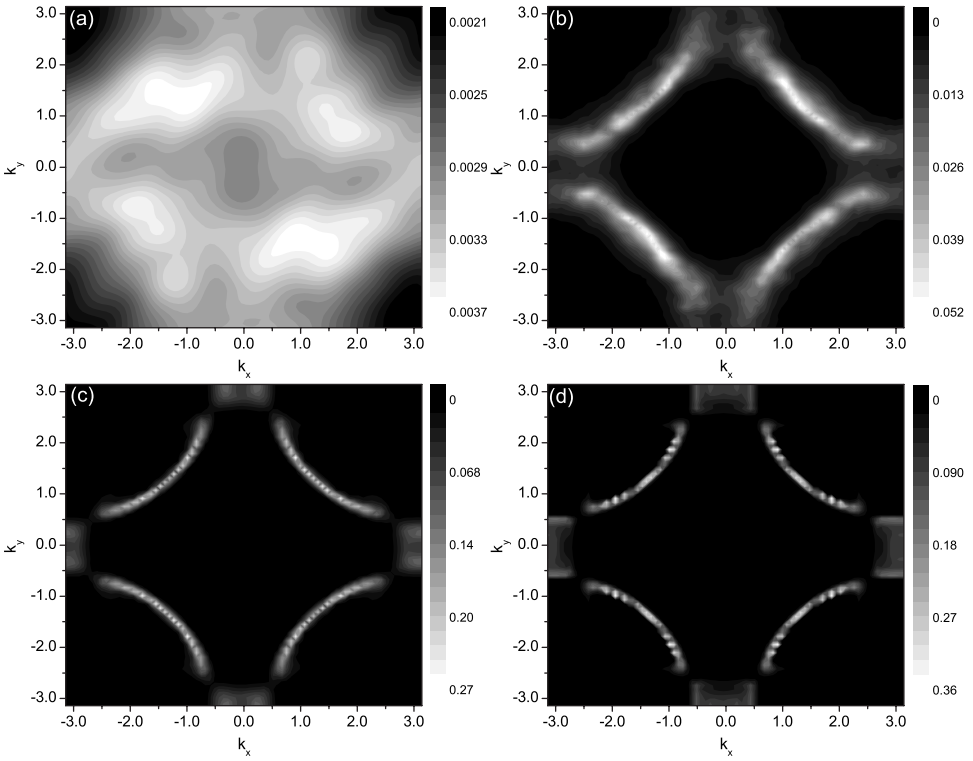

FIG. 2. The spectral function $A(\mathbf{k},\omega=\mu)$ for $g_V/(2\pi)=0.1t$. The correlation lengths are $l_D=0$, 2, 8, and 16 from panels (a) through (d), respectively. The remaining parameters are given in the text.

tonian on a square lattice in a sample of dimension $N\times M$, with the lattice constant set to unity, is

$$H=\sum_{\mathbf{i}}\epsilon_{\mathbf{i}}c_{\mathbf{i}}^{\dagger}c_{\mathbf{i}}+\sum_{\mathbf{i},\mathbf{j}}t_{\mathbf{i},\mathbf{j}}e^{ia_{\mathbf{i},\mathbf{j}}}c_{\mathbf{i}}^{\dagger}c_{\mathbf{j}}+\text{H.c.}, \tag{9}$$

where $c_{\mathbf{i}}$ is the fermionic annihilation operator at the site $\mathbf{i}$. The spin degrees of freedom are omitted for simplicity. The hopping amplitude $t_{\mathbf{i},\mathbf{j}}$ vanishes except for nearest and next-nearest neighbors. To include twofold commensurate DDW order, the nearest-neighbor hopping amplitudes are chosen to be

$$t_{\mathbf{i},\mathbf{i}+\hat{\mathbf{x}}}=-t+\frac{iW_0}{4}(-1)^{(n+m)},$$

$$t_{\mathbf{i},\mathbf{i}+\hat{\mathbf{y}}}=-t-\frac{iW_0}{4}(-1)^{(n+m)}, \tag{10}$$

where (n,m) are a pair of integers labeling a site: $\mathbf{i}=n\hat{\mathbf{x}}+m\hat{\mathbf{y}}$, and W_0 is the DDW gap; for the next-nearest hopping $t_{\mathbf{i},\mathbf{j}}=t'$. The on-site impurity energy $\epsilon_{\mathbf{i}}$ is defined by

$$\epsilon_{\mathbf{i}}=\frac{V_0}{Z}\sum_{\mathbf{r}}G_{\mathbf{r}}e^{-|\mathbf{r}-\mathbf{i}|^2/2l_D^2}, \tag{11}$$

which is analogous to Eq. (4). To model correlated disorder, we set the disorder averages $\langle G_{\mathbf{r}}\rangle=0$ and $\langle G_{\mathbf{r}}G_{\mathbf{r}'}\rangle=\delta_{\mathbf{r},\mathbf{r}'}$, and

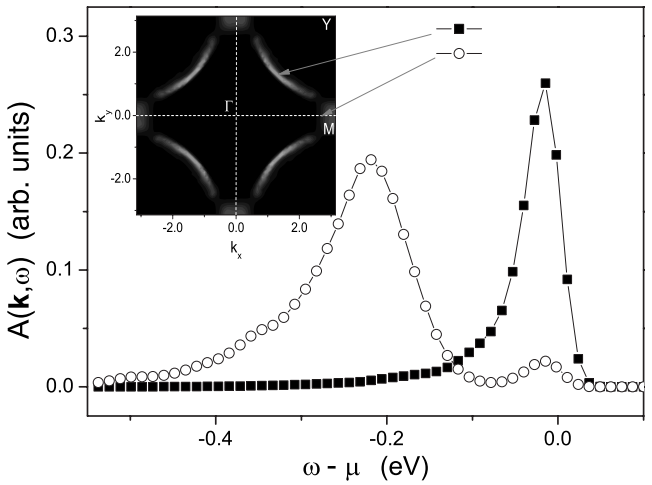

FIG. 3. The energy dependence of the spectral function $A(\mathbf{k},\omega)$ at two $\mathbf{k}$ points in the Brillouin zone, as indicated in the inset.

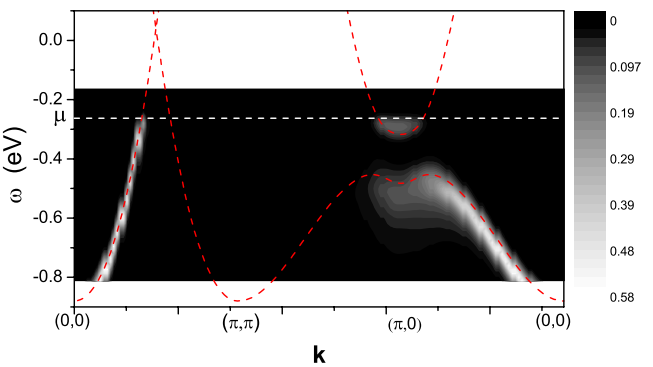

FIG. 4. (Color online) The gray scale plot of the spectral function $A(\mathbf{k},\omega)$ as a function of both $\mathbf{k}$ and ω. Dashed curves indicate the quasiparticle dispersion relation. A horizontal dashed line shows the chemical potential μ. The remaining parameters are given in the text.

$Z=\Sigma_{\mathbf{r}}e^{-|\mathbf{r}|^2/2l_D^2}$ is a normalization factor. V_0 parameterizes the disorder intensity. Note that Eq. (11) reduces to $\epsilon_{\mathbf{i}}=V_0G_{\mathbf{i}}$ in the limit $l_D\to 0$ and $\epsilon_{\mathbf{i}}$ becomes uncorrelated random variables. A constant perpendicular magnetic field B is included via the Peierls phase factor $a_{\mathbf{i},\mathbf{j}}=\frac{2\pi e}{h}\int_{\mathbf{j}}^{\mathbf{i}}\mathbf{A}\cdot d\mathbf{l}$, where $\mathbf{A}=(0,-Bx,0)$ is the vector potential in the Landau gauge. We note that a perpendicular magnetic field even as large as 60 T has little effect on DDW order.[31]

In this section we choose $t=0.29$ eV, $t'=0.1$ eV, and $W_0=0.065$ eV. The chemical potential is set to be $\mu=-0.28$ eV. Note that these parameters are slightly different from those in the previous section, although the hole doping is again $\sim 10\%$. We have left out the third-nearest-neighbor hopping, which greatly complicates the transfer-matrix calculation without offering any particular insight. The disorder intensity $V_0=0.4t$ leads to a quasiparticle lifetime on the order of $\sim 10^{-12}$ s in the limit of $l_D=0$. The magnetic field ranges from $B=20$ T to $B=75$ T, representative of the quantum-oscillation experiments. The only relevant length scale here is the magnetic length $l_B=\sqrt{\hbar/eB}$, which for $B=20$ T is $\sim 15a$, a being lattice constant equal to 3.85 Å.

Now consider a quasi-one-dimensional system, $N\gg M$ with a periodic boundary condition along y direction. Let $\Psi_n=(\psi_{n,1},\psi_{n,2},\ldots,\psi_{n,M})^T$ be the amplitudes on the slice n for an eigenstate with a given energy E, then the amplitudes on three successive slices satisfy the relation

$$\begin{bmatrix}\Psi_{n+1}\\ \Psi_n\end{bmatrix}=\begin{bmatrix}T_n^{-1}(E-H_n) & -T_n^{-1}T_{n-1}\\ 1 & 0\end{bmatrix}\begin{bmatrix}\Psi_n\\ \Psi_{n-1}\end{bmatrix}, \quad (12)$$

where H_n is the Hamiltonian within the slice n and the matrix T_n corresponds to the hopping between the slices n and $n+1$. T_n is tridiagonal, as electrons can hop from a site on slice n to three sites on the slice $n+1$. All postive Lyapunov exponents of the transfer matrix,[32] $\gamma_1>\gamma_2>\cdots>\gamma_M$, are computed by iterating Eq. (12) and performing orthonormalization regularly. The convergence of this algorithm is guaranteed by the well-known Oseledec theorem.[33] For the above parameters a transverse dimension corresponding to $M=40$ is sufficient. Equation (12) was iterated 10^5-10^6 times until the relative errors of less than 1% of all the Lyapunov exponents were achieved.

B. Computation of σ_{xx}

The conductivity σ_{xx} at zero temperature is obtained from the Landauer formula[34–36]

$$\sigma_{xx}(B)=\frac{e^2}{h}\sum_{i=1}^{M}\frac{1}{\cosh^2(M\gamma_i)}. \quad (13)$$

The SdH oscillations of σ_{xx} at zero temperature for $l_D=0$ is shown in the inset of Fig. 5. A third-order polynomial was used to subtract the background. The Fourier transform is shown in the main panel of Fig. 5. Clearly, there are two main oscillation frequencies $F_1=490\pm 30$ T and $F_2=900\pm 30$ T, corresponding to electron and hole pockets, respectively, although a few harmonics are also visible. Though the first peak at F_1 agrees with experimental observations, the second peak at F_2 has not yet been observed.

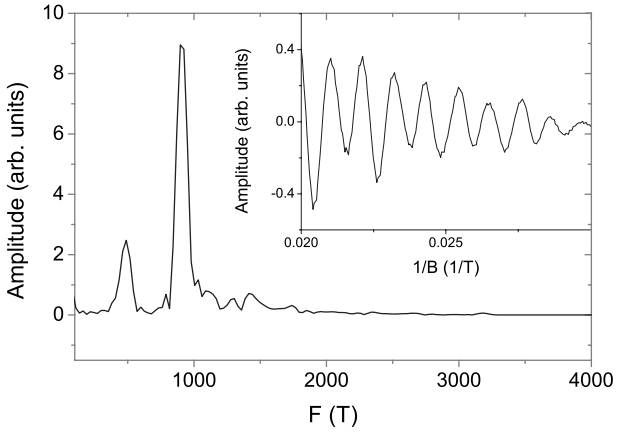

FIG. 5. Fourier transform of SdH oscillations at zero temperature for $l_D=0$ in arbitrary units. Inset shows oscillations as a function of the inverse magnetic field. Note the presence of higher harmonics. The parameters are described in the text.

For correlated disorder, the Fourier transform of σ_{xx} is plotted in Fig. 6. In all the cases, two main frequencies of $F_1\sim 500$ T and $F_2\sim 900$ T are prominent. As for $A(\mathbf{k},\omega)$, an increase in l_D increases the amplitudes of F_1 and F_2, because the effective disorder becomes weaker with the increased correlation length. Also the higher harmonics are more visible. There is, however, a sharp distinction between the dependence of the two physical quantities, which becomes clear when we consider the white-noise case: $A(\mathbf{k},\omega)$ is completely smeared out in the momentum space because white-noise scatters between all possible wave vectors; see Fig. 2(a). The coherence factors are of crucial importance for the spectral function. In contrast, the SdH oscillations are damped by the Dingle factor, which is parametrized by a single lifetime and disorder enters in an averaged sense. This striking contrast is clear in Fig. 5. The surprise is that impurity scattering affects the electron pocket more than the hole pocket, which is remarkably robust even for white noise. There must be a piece of physics missing, if we are to explain why the hole pocket is not observed in SdH. This missing physics we argue is the vortex scattering rate which affects the two pockets very differently.

IV. VORTEX SCATTERING RATE IN THE MIXED STATE

We have shown previously[9] that the scattering rate of the DDW quasiparticles, corresponding to the electron pockets from vortices in the mixed state is given by,

$$\left(\frac{1}{\omega_c\tau_v}\right)_e\approx\frac{\Delta^2}{\hbar}\sqrt{\frac{\pi}{|\mu|\hbar\omega_c^3}}, \quad (14)$$

where the cyclotron frequency ω_c is determined from the band mass m_b to be (restoring the lattice spacing a here)

$$\frac{\hbar^2}{2m_b}\approx\left(2t'+4t''-\frac{W_0}{4}\right)a^2. \quad (15)$$

Here Δ^2, a measure of the amplitude of the superconducting gap, is an average over the disordered configuration of the

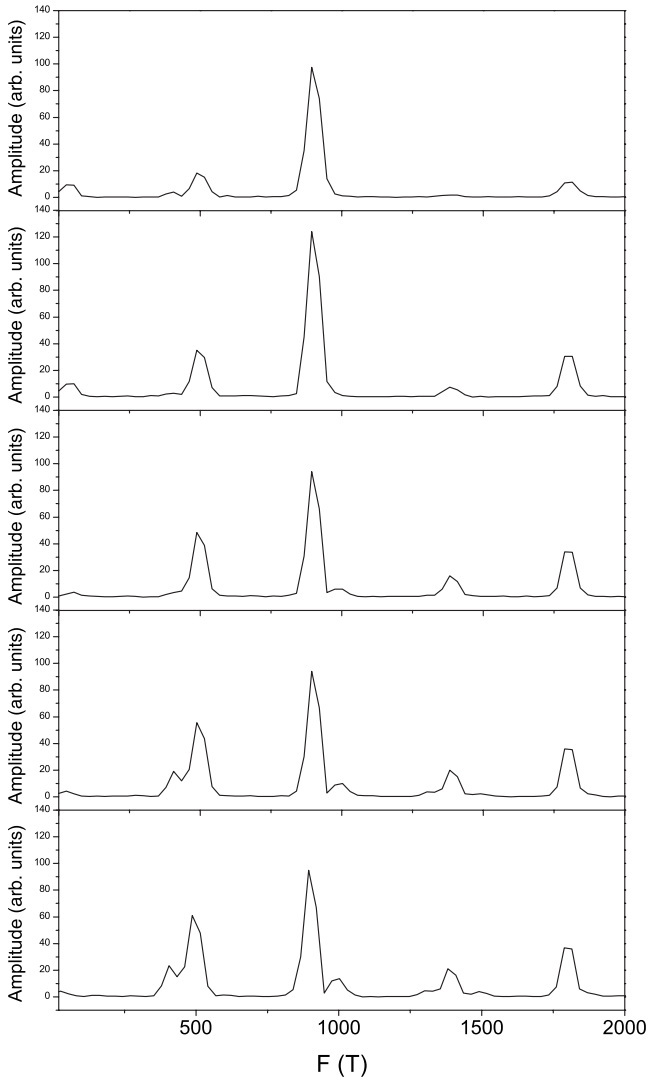

FIG. 6. Fourier transform of SdH oscillations for correlated disorder at zero temperature. The correlation length $l_D=1$, 2, 4, 8, and 16 for panels (a) through (e), respectively. The remaining parameters are described in the text.

vortices, which is likely to be insensitive to the symmetry of the order parameter. Similarly, we have shown that the vortex scattering rate for the nodal DDW quasiparticles at the hole pocket is given by (noting a typographical error in Ref. 9)

$$\left(\frac{1}{\tau_v}\right)_h \approx \frac{\Delta^2}{\hbar}\frac{\sqrt{2\pi}}{\sqrt{|\mu|\hbar\omega_c^*}}. \tag{16}$$

The relevance of nodal quasiparticle dispersion is also pointed out in Ref. 13. We have introduced a characteristic mass and a frequency scale by (nodal quasiparticle are actually massless)

$$m^* = \frac{|\mu|}{v_F v_D}, \tag{17}$$

$$\omega_c^* = \frac{eB}{m^* c}. \tag{18}$$

The reason for this is that these are precisely the scales that enter a SdH calculation of the nodal quasiparticles.[37] It can be seen from the above equations that the vortex scattering rate for the nodal particles is proportional to $1/\sqrt{W_0}$. This diverges as $W_0 \to 0$. But this is not unphysical, as, in that limit, there is a phase transition, where the Fermi-surface reconnects.[17] The nodal fermions are obviously no longer a valid description. However, our mean-field theory cannot be trusted to predict the precise scattering rate at this quantum critical point. We have restricted ourselves to a regime that we believe is deep inside the broken-symmetry phase where our treatment should be a good guide, and where we believe that the present experiments are performed. A proper treatment of this scattering rate at the point where W_0 collapses is an open question that may shed light to the physics of the striking strange metal phase.

The physical picture underlying the calculation of Stephen[29] is that the lifetime obtained from the imaginary part of the self-energy corresponds to a situation as if the vortices are static impurities. Here $v_F=2\sqrt{2}at/\hbar$ is the magnitude of the velocity in a direction normal to the hole pocket and $v_D=W_0 a/\sqrt{2}\hbar$ is the velocity in a direction orthogonal to it; neither t' nor t'' enter in the leading order. Therefore,

$$\left(\frac{1}{\omega_c^*\tau_v}\right)_h \approx \sqrt{2}\left(\frac{m^*}{m_b}\right)^{3/2}\left(\frac{1}{\omega_c\tau_v}\right)_e \tag{19}$$

The cancellation of Δ^2 is interesting but cannot of course be an exact result considering the approximations involved in Stephen's analysis.[29] The correctness of which relies entirely on the formulation of the averaged Green's function of Stephen, where this average is carried out in the real space, and the nature of the normal state (whether or not it contains electron and hole pockets in the momentum space) does not enter, as the normal-state Green's function does not contain the superconducting order parameter. On the other hand, we had roughly estimated $m_b \approx 1.27 m_e$ and $m^* \approx 2.72 m_e$ for a typical set of parameters,[9] where m_e is the free-electron mass. Thus, it is reasonable that

$$\left(\frac{1}{\omega_c^*\tau_v}\right)_h \approx 4.4\left(\frac{1}{\omega_c\tau_v}\right)_e, \tag{20}$$

which should be robust with respect small changes in the band parameters and the DDW gap. This would lead to a strong suppression of the oscillations corresponding to the hole pocket as compared to the electron pocket, as the Dingle factors, $\mathcal{D}_{e,h}$ are exponentially sensitive to the product of the cyclotron frequency and the vortex scattering lifetime: $\mathcal{D}_e = e^{-\pi/(\omega_c\tau_v)_e}$ and $\mathcal{D}_h = \mathcal{D}_e^{4.4}$. The previously estimated lifetime of the electrons,[9]

$$\left(\frac{1}{\tau_v}\right)_e = 1.5 \times 10^{12}\ \text{s}^{-1}, \tag{21}$$

for $B=40$ T and $B_{c2}=60$ T should be a rough guide.

The whole analysis is predicated on the assumption that the quantum-oscillation frequencies are unshifted from the

putative normal state (the DDW state in this case), for which we now provide some support from the analysis of Stephen;[29] see, however Ref. 38. The formula for the relative frequency shift in terms of physical parameters (absolutely essential because they are all effective parameters) is

$$\frac{\Delta F}{F} = \frac{\pi}{8}\frac{\Delta(H)^4}{\hbar\omega_c|\mu|^3}, \tag{22}$$

where $\Delta(H)$ is the zero-temperature superconducting gap in a magnetic field; for a d-wave superconductor we have to use an appropriate average, as above. The factor $\hbar\omega_c$ for free electrons is given by

$$\hbar\omega_c = 1.34 \times 10^{-4} \times H \ \text{(T)eV}. \tag{23}$$

As will be seen below, it will make little difference if we use the mass determined from experiments. The magnetic field ranges between 30 and 65 T. Let us take $H=40$ T. Then

$$\hbar\omega_c = 5.36 \times 10^{-3} \ \text{eV}. \tag{24}$$

We know little about the zero-temperature gap, especially in the underdoped regime, where there are fluctuation effects. As the simplest assumption, we use BCS mean-field theory,

$$\Delta(H) = \Delta(0)\sqrt{1 - H/H_{c2}} \tag{25}$$

and $2\Delta(0)=3.52T_c$, which results in

$$\Delta(0) = 8.6 \ \text{meV} \tag{26}$$

for $T_c=57.5$ K.[1,2] For simplicity we choose $\Delta(0)\approx 10$ meV, and as a rough guide from experiments,[1,2] $H_{c2}\approx 60$ T, although it will make little difference even if it were 100 T. For 10% doping we need a chemical potential $\mu\approx -0.26$ eV. Thus, we get

$$\frac{\Delta F}{F} = 4.6 \times 10^{-6}. \tag{27}$$

Even if this estimate were incorrect by several orders of magnitude, our conclusions that the frequency shift is negligible should be valid.

Consider the white noise as an example; see Fig. 5. We first filter out the two peaks, invert the Fourier transform, and then multiply by the Dingle factors corresponding to the vortex scattering rates discussed in this section. Using Eqs. (20) and (21) and Fourier transforming back this procedure essentially wipes out the peak corresponding to the frequency of hole pocket in the resulting transform, as shown in Fig. 7.

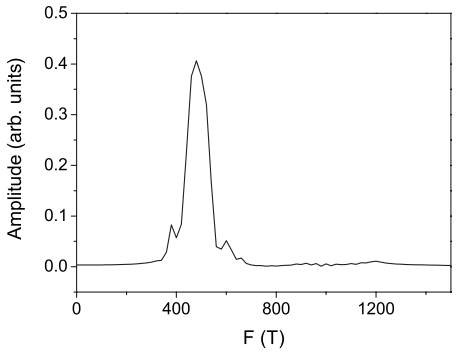

FIG. 7. Fourier transform of SdH oscillations shown in Fig. 5, after taking into account vortex scattering rates in the mixed state, as discussed in the text. Note that the amplitude of the peak corresponding to the hole pocket at about 900 T is essentially wiped out.

V. CONCLUSIONS

In summary, we have shown that two of the most puzzling features in underdoped cuprates, the nonexistence of electron pockets in ARPES and the lack evidence of the hole pockets in quantum oscillations can be plausibly resolved by considering correlated disorder and the vortex scattering rates in the mixed state. With respect to the latter, it is crucial that the nodal fermions are described by a relativistic spectrum while the quasiparticles corresponding to the electron pocket are described by a nonrelativistic spectrum determined by the bottom of the band.

It is important to determine if the calculation of Stephen can be so closely taken over after modifying for the presence of nodal fermions. We believe that it can be because the relative frequency shift turns out to be very small, on the order of 10^{-6}. Thus, even if the estimate is off by some orders of magnitude, we still have enough leeway. This argument has been recently challenged[38] in a calculation of the density of states, however. Clearly, further investigations will be extremely valuable and are in progress.

One of the surprising conclusions of the present work, which we believe is on firm grounds, is that even very strong disorder, such as white noise, has only a modest effect on quantum oscillations, while it has a much larger effect on the ARPES spectra. This is because ARPES spectral function depends on the coherence factors, which act as Wannier functions that are naturally very sensitive to disorder. In quantum-oscillations disorder appears primarily as an averaged lifetime in the Dingle factor. Elastic scattering has little direct effect on the Onsager quantization condition.

It is also a firm conclusion of our work that elastic disorder scattering from impurities cannot be responsible for wiping out the hole-pocket frequency while keeping the electron pocket frequency more or less intact. In fact, quite the opposite seems to be true. Thus, the vortex physics in the mixed state appears to be of paramount importance, especially the contrast between the nonrelativistic electrons around the antinodal point and the relativistic nodal fermions at the nodal points of the Brillouin zone.

We also note an interesting paper[39] regarding an analysis of various masses involved, which take into account electron-electron interactions. In the future, it would be interesting to pursue such an analysis of residual electron-electron interactions in the present context.

ACKNOWLEDGMENTS

This work is supported by NSF under Grant No. DMR-0705092. We thank Patrick Lee for many clarifying discussions.

[1] N. Doiron-Leyraud, C. Proust, D. LeBoeuf, J. Levallois, J.-B. Bonnemaison, R. Liang, D. A. Bonn, W. N. Hardy, and L. Taillefer, Nature (London) **447**, 565 (2007).
[2] D. LeBoeuf, N. Doiron-Leyraud, J. Levallois, R. Daou, J. B. Bonnemaison, N. E. Hussey, L. Balicas, B. J. Ramshaw, R. Liang, D. A. Bonn, W. N. Hardy, S. Adachi, Cyril Proust, and Louis Taillefer, Nature (London) **450**, 533 (2007).
[3] A. F. Bangura, J. D. Fletcher, A. Carrington, J. Levallois, M. Nardone, B. Vignolle, P. J. Heard, N. Doiron-Leyraud, D. LeBoeuf, L. Taillefer, S. Adachi, C. Proust, and N. E. Hussey, Phys. Rev. Lett. **100**, 047004 (2008).
[4] C. Jaudet, D. Vignolles, A. Audouard, J. Levallois, D. LeBoeuf, N. Doiron-Leyraud, B. Vignolle, M. Nardone, A. Zitouni, R. Liang, D. A. Bonn, W. N. Hardy, Louis Taillefer, and Cyril Proust, Phys. Rev. Lett. **100**, 187005 (2008).
[5] E. A. Yelland, J. Singleton, C. H. Mielke, N. Harrison, F. F. Balakirev, B. Dabrowski, and J. R. Cooper, Phys. Rev. Lett. **100**, 047003 (2008).
[6] S. E. Sebastian, N. Harrison, E. Palm, T. P. Murphy, C. H. Mielke, R. Liang, D. A. Bonn, W. N. Hardy, and G. G. Lonzarich, Nature (London) **454**, 200 (2008).
[7] S. Chakravarty and H.-Y. Kee, Proc. Natl. Acad. Sci. U.S.A. **105**, 8835 (2008).
[8] X. Jia, I. Dimov, P. Goswami, and S. Chakravarty, arXiv:0806.3793 (unpublished).
[9] I. Dimov, P. Goswami, X. Jia, and S. Chakravarty, Phys. Rev. B **78**, 134529 (2008).
[10] A. J. Millis and M. R. Norman, Phys. Rev. B **76**, 220503(R) (2007).
[11] D. Podolsky and H.-Y. Kee, Phys. Rev. B **78**, 224516 (2008).
[12] J. Lin and A. J. Millis, Phys. Rev. B **78**, 115108 (2008).
[13] T. Morinari, J. Phys. Soc. Jpn. **78**, 054708 (2009).
[14] S. Chakravarty, Science **319**, 735 (2008).
[15] A. Damascelli, Z. Hussain, and Z.-X. Shen, Rev. Mod. Phys. **75**, 473 (2003).
[16] M. A. Hossain, J. D. F. Mottershead, D. Fournier, A. Bostwick, J. L. McChesney, E. Rotenberg, R. Liang, W. N. Hardy, G. A. Sawatzky, I. S. Elfimov, D. A. Bonn, and A. Damascelli, Nat. Phys. **4**, 527 (2008).
[17] S. Chakravarty, R. B. Laughlin, D. K. Morr, and C. Nayak, Phys. Rev. B **63**, 094503 (2001).
[18] S. Tewari, H.-Y. Kee, C. Nayak, and S. Chakravarty, Phys. Rev. B **64**, 224516 (2001).
[19] S. Chakravarty, C. Nayak, S. Tewari, and X. Yang, Phys. Rev. Lett. **89**, 277003 (2002).
[20] S. Tewari and C. Zhang, Phys. Rev. Lett. **103**, 077001 (2009).
[21] C. Nayak, Phys. Rev. B **62**, 4880 (2000).
[22] C. Nayak and E. Pivovarov, Phys. Rev. B **66**, 064508 (2002).
[23] U. Schollwöck, S. Chakravarty, J. O. Fjærestad, J. B. Marston, and M. Troyer, Phys. Rev. Lett. **90**, 186401 (2003).
[24] H. A. Mook, P. Dai, S. M. Hayden, A. Hiess, J. W. Lynn, S. H. Lee, and F. Doğan, Phys. Rev. B **66**, 144513 (2002).
[25] H. A. Mook, P. Dai, S. M. Hayden, A. Hiess, S. H. Lee, and F. Doğan, Phys. Rev. B **69**, 134509 (2004).
[26] C. Stock, W. J. L. Buyers, Z. Tun, R. Liang, D. Peets, D. Bonn, W. N. Hardy, and L. Taillefer, Phys. Rev. B **66**, 024505 (2002).
[27] B. Fauqué, Y. Sidis, V. Hinkov, S. Pailhes, C. T. Lin, X. Chaud, and P. Bourges, Phys. Rev. Lett. **96**, 197001 (2006).
[28] It is important to exercise some caution. It has been argued in Refs. 24 and 25 that it is crucial to perform polarized neutron-scattering to detect signatures of DDW. The reason is that large samples necessary for magnetic neutron-scattering contain much spurious signal that need to be filtered out by polarized measurements from the very small signals due to DDW order. It is also important to perform an analysis of the form factor as a function of L at the reciprocal space (H,K,L) (expressed in terms of reciprocal-lattice units). The form factor can reveal if the scattering is from orbital moments that are more spread out in the real space in contrast to scattering from pointlike localized spin moments, perhaps parasitical. None of these were performed in Ref. 26. As to Ref. 27, no data exhibiting nonexistence of DDW are presented.
[29] M. J. Stephen, Phys. Rev. B **45**, 5481 (1992).
[30] S. Chakravarty, C. Nayak, and S. Tewari, Phys. Rev. B **68**, 100504(R) (2003).
[31] H. K. Nguyen and S. Chakravarty, Phys. Rev. B **65**, 180519(R) (2002).
[32] B. Kramer and M. Schreiber, in *Computational Physics*, edited by K. H. Hoffmann and M. Schreiber (Springer, Berlin, 1996), p. 166.
[33] V. Oseledec, Trans. Mosc. Math. Soc. **19**, 197 (1968).
[34] D. S. Fisher and P. A. Lee, Phys. Rev. B **23**, 6851 (1981).
[35] H. U. Baranger and A. D. Stone, Phys. Rev. B **40**, 8169 (1989).
[36] B. Kramer and A. MacKinnon, Rep. Prog. Phys. **56**, 1469 (1993).
[37] P. Goswami, X. Jia, and S. Chakravarty, Phys. Rev. B **78**, 245406 (2008).
[38] K.-T. Chen and P. A. Lee, Phys. Rev. B **79**, 180510(R) (2009).
[39] T. D. Stanescu, V. Galitski, and H. D. Drew, Phys. Rev. Lett. **101**, 066405 (2008).